Measurement and numerical studies of optical properties of YAG:Ce phosphor for white light-emitting diode packaging

Zongyuan Liu,[1,2] Sheng Liu,[1,2,*] Kai Wang,[2,3] and Xiaobing Luo[2,4]

[1]School of Mechanical Science and Engineering, Huazhong University of Science and Technology, Wuhan 430074, China

[2]MOEMS Division, Wuhan National Laboratory for Optoelectronics, Wuhan 430074, China

[3]School of Optoelectronics Science and Engineering, Huazhong University of Science and Technology, Wuhan 430074, China

[4]School of Energy and Powering Engineering, Huazhong University of Science and Technology, Wuhan 430074, China

*Corresponding author: victor_liu63@126.com

Received 13 July 2009; accepted 15 November 2009;
posted 3 December 2009 (Doc. ID 113394); published 8 January 2010

The optical properties of YAG:Ce phosphor were measured by a double-integrating-sphere system and calculated by Mie theory and Monte Carlo ray tracing to provide precise optical characterizations of YAG:Ce phosphor for white light-emitting diode (LED) packaging design. Measurement results showed that the phosphor presents strong absorption for blue light, high reflection for yellow light, and an isotropic emission pattern of converted light. The conversion efficiency and quantum efficiency for the saturated phosphor are around 70% and 87%, respectively. Based on the measurement results, the absorption coefficient, scattering coefficient, and anisotropy factor of the phosphor calculated by Mie theory were compared with those calculated by ray-tracing simulation to modify Mie theory to find a reasonable method that can easily obtain the optical constants of YAG:Ce phosphor. Comparisons revealed that Mie theory can predict the variation of the optical constants of phosphor, but the absorption and scattering cross sections should be multiplied with two fitting parameters. The fitting parameters have been given in this study and can be obtained by testing packaged LEDs with different phosphor concentrations.

OCIS codes: 120.4530, 160.2540, 290.5820, 290.4020, 290.5850, 230.3670.

1. Introduction

White light-emitting diodes (LEDs) have been characterized as the future illumination styles to replace traditional light sources due to their superior features, such as small size, low power consumption, high efficiency, long life, and variable color [1–4]. Phosphor-converted LED (pcLED) is one of the most promising technologies to obtain high-quality white LEDs [5–7]. This promotes the rapid development of phosphor materials, including Ce^{3+}-doped garnet materials [8] and Eu^{2+}-activated nitride and silicate compounds [9–11]. Among these materials, YAG:Ce phosphor currently presents the highest quantum efficiency, the best optical-thermal stability [12], and the widest waveband [9], and is, therefore, chosen for the generation of natural and cool white LEDs. The multiphosphor converted warm white LEDs also prefer YAG:Ce phosphor to be the yellow–green spectra converter to increase the luminous efficiency.

However, the packaging issues caused by phosphor materials and the further penetration of white LEDs into general illumination demand a profound

0003-6935/10/020247-11$15.00/0

understanding of the optical properties of phosphor [13]. Previous studies have revealed that phosphor optical properties have remarkable impacts on LED packaging performance, such as light extraction [14–20], spatial color distribution [21,22], and color quality [7,9]. These studies normally apply the Monte Carlo method for the optical simulation of LED packaging, in which the phosphor layers were considered to be Mie scattering materials. The issue is that the optical definitions of the phosphor in these simulations suffered from lack of precise phosphor optical constants verified by experiments. Most of studies about YAG:Ce phosphor focused on the photoluminescence and the excitation and emission spectra, and lacked a substantial consideration of the light scattering, which is essential for white LED packaging. Narendran *et al.* [18], Zhu *et al.* [23], and Kang *et al.* [24] tested the optical properties of YAG:Ce phosphor and presented improved packaging methods based on their studies. The issues are that the phosphor layer in [23] was not a uniform film, in [24] it was coated on the chip for test, and the incident light in [18] was divergent and can result in high reflection. These issues affected the true performance of the phosphor. In addition, the optical constants of the phosphor were not clearly given in [18,23,24]. This causes the further research of LED packaging design to be difficult. Therefore, it is important to develop an improved measurement platform and determine the optical constants of YAG:Ce phosphor by numerical analysis.

A double-integrating-sphere system has been used extensively for the measurement of bulk scattering materials [25,26]. This system collects the transmitted light and reflected light for the tested materials and then obtains the optical constants by numerical calculations. Mie theory is one of the most adopted theories. Considering that YAG:Ce phosphor is a fluorescent material and will present some features unlike those of traditional scattering materials, this paper applied a Monte Carlo ray tracer to examine the Mie theoretical results and determined the optical constants by ray-tracing simulation. Section 2 introduces the measurement platform and the experimental method for YAG:Ce phosphor based on its photoluminescence properties. Section 3 presents the measurement results and a short discussion about the effects of the phosphor properties on LED packaging. In Section 4, a detailed Mie theoretical calculation is given and then modified by Monte Carlo ray-tracing simulation. In Section 5, by modifying the absorption and scattering cross sections of the phosphor, a revised Mie calculation method of the optical constant of YAG:Ce phosphor is proposed to facilitate the optical design of white LEDs.

2. Description of Measurement Platform

As shown in Fig. 1, the measurement platform is a double-integrating-sphere system with a parallel incident light source to excite YAG:Ce phosphor. Before the measurement, the fluorescence of the phosphor has been tested by a spectrofluorimeter, FP-6500 from Jasco, as shown in Fig. 2. In white LED packaging, the main concerns are the absorption and scattering properties of YAG:Ce phosphor for blue light emitted from the chip and converted light emitted from itself. Therefore, the measurement platform used two color LEDs with peak wavelengths of 455 and 595 nm as the light sources. Diameters of the two integrating spheres are 150 mm. Diameters of the apertures are 30 mm. The phosphor slide was composed of a 2 in. (5 cm) diameter glass and a thin phosphor film. The thickness of the glass is 0.9 mm. To fabricate the phosphor film, the first step was dispensing the mixture of YAG:Ce phosphor powder and silicone on one glass slide with two spacers. Then, another glass slide precoated with Teflon was pressed on the mixture, the thickness of which was limited by the two spacers. This glass was removed after the curing of the phosphor silicone. The thickness of the phosphor films was changed from 0.06 to 0.3 mm, and the concentration was changed from 0.2 to 0.5 g/cm^3. A spectrophotometer, PMS-50 from Everfine, was used to test the transmitted light spectra and reflected light spectra with the light power converted by a photomultiplier tube. The benefits of this measurement platform are that the influences of chip absorption and phosphor shape on the phosphor properties have been reduced to the minimum and the parallel incident light can avoid the potential test errors by divergent incident light [18].

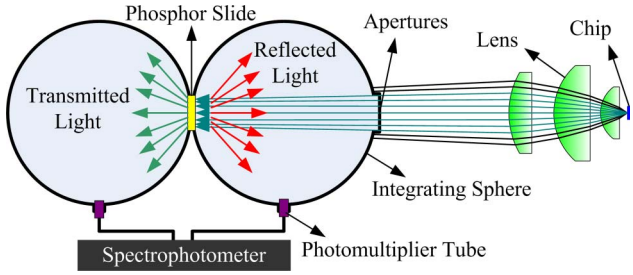

Fig. 1. (Color online) Measurement platform of YAG:Ce phosphor.

For blue light (455 nm) excitation, the spectra of transmitted light and reflected light are divided into

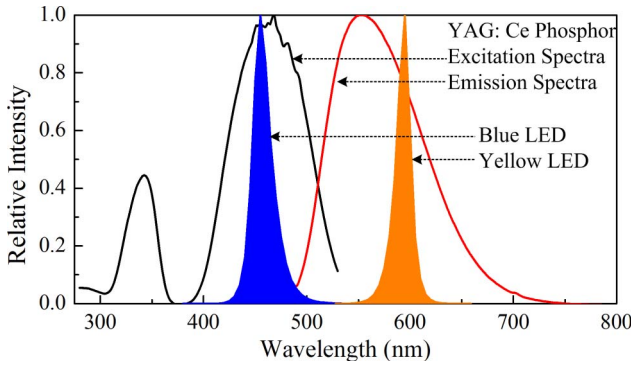

Fig. 2. (Color online) Excitation and emission spectra of YAG:Ce phosphor, and the spectra of blue LED and yellow LED used in this study.

two parts at 490 nm. Light with spectra from 380 to 490 nm is defined as unconverted blue light, and light with spectra from 490 to 780 nm is defined as converted light. For yellow light (595 nm) excitation, since no converted light is emitted from the phosphor film, both the transmitted light and reflected light are sorted as the yellow light. The total optical power of the blue light and the yellow light was tested before the adding of the phosphor slide in the aperture, and are denoted as P_{total}. The optical power of transmitted light and reflected light are denoted as P_T and P_R. This study sets the transmittance and reflectance as the ratios of P_T to P_{total} and P_R to P_{total}, respectively.

3. Results and Discussions

The experimental results are displayed in Fig. 3. For simplicity, the reflectance and transmittance for the unconverted blue light (455 nm) and the yellow light (595 nm) are denoted as η_{BR}, η_{BT}, η_{YR}, and η_{YT}, and the converted light from phosphor are denoted as η_{CR} and η_{CT}.

Comparing Fig. 3(a) with Fig. 3(b), it can be found that the YAG:Ce phosphor presents remarkable high absorption for the blue light and causes rapid attenuation of η_{BT} and small reduction of η_{BR} when the phosphor thickness and the concentration increase. With the increase of the phosphor thickness and the concentration, η_{YT} is also reduced, but η_{YR} is increased quickly. This is mainly because, during the light propagation, the backward-scattered blue light is further absorbed by the phosphor particles, whereas the backward-scattered yellow light can emit out due to the weak absorption of the phosphor. Therefore, in white LED packaging, once the blue light emits out of the chip, the light loss caused by the chip absorption will be small. Oppositely, since most of the extracted blue light is absorbed by the phosphor, the high η_{YR} can affect the light extraction significantly by the multiple reflection of the converted light between the phosphor layer and the chip. In traditional white LED packaging, with the phosphor directly coated on the chip surface, this multiple reflection can result in high chip absorption for the converted light. Therefore, the luminous efficiency will be reduced and the LED color will tend to be high correlated color temperature (CCT).

The emission performance of the converted light of YAG:Ce phosphor in Fig. 3(c) is another reason affecting LED packaging performance. It can be found that η_{CT} and η_{CR} present similar values and tendencies as the phosphor thickness and the concentration increase. This indicates that the emission pattern of a phosphor particle may be isotropic. To better understand the conversion and emission behaviors of the phosphor, the conversion efficiency η_{CE} and the ratio of η_{CT} to η_{CR} are shown in Fig. 4. Results reveal that η_{CE} of the saturated phosphor is slightly higher than 70% and $\eta_{\text{CT}}/\eta_{\text{CR}}$ is approximately 1.05–1.15. According to [15], the conversion efficiency is a multiplication of the Stokes efficiency and the quantum efficiency of the phosphor. The dominant wavelength of the converted light is approximately 562 nm. Therefore, the Stokes efficiency is around 81% and the quantum efficiency is around 87%. For cases with low concentration and thin thickness, the unsaturated phosphor demonstrates lower η_{CE}. If the thickness is too thick or the concentration is too high, the oversaturated phosphor causes more converted light to be backreflected. In white LED packaging, the low η_{CE} is the intrinsic property of the phosphor and can only be improved by the quantum efficiency. However, the isotropic emission pattern of the converted light means that approximately half of the converted light must suffer the multiple reflection between the phosphor layer and the chip. A rough

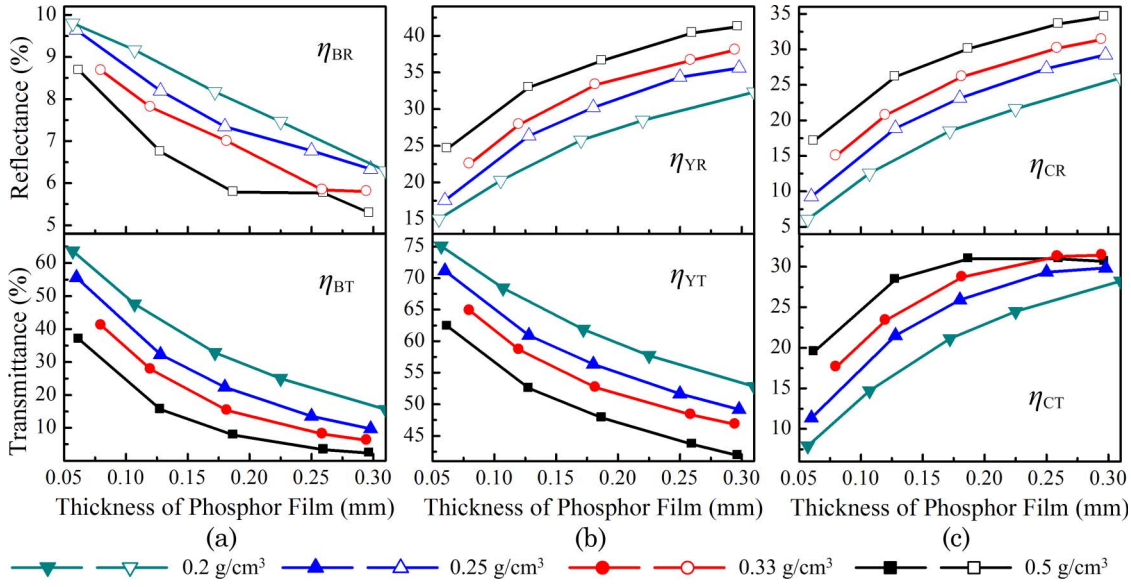

Fig. 3. (Color online) Measurement results of the reflectance and transmittance of YAG:Ce phosphor samples for (a) blue light from blue LED, (b) yellow light from yellow LED, and (c) converted light from the phosphor.

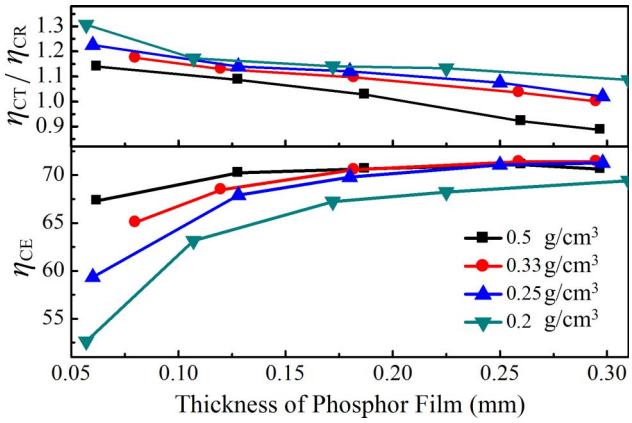

Fig. 4. (Color online) Emission and conversion properties of YAG:Ce phosphor.

estimation of 25% of the converted light will be lost due to the chip absorption during the multiple reflection for the traditional white LEDs.

Therefore, the traditional packaging method is not an ideal packaging configuration for light extraction. If the reflected portion of the converted light can be totally extracted by reducing the light loss caused by the chip absorption and other factors to obtain an ideally packaged white LEDs, for example, the planar remote phosphor packaging [14], the hemispherical remote phosphor packaging [17], and the LED coated with a photonic crystal layer [20], a theoretical estimation for the improvement of light extraction can be as high as 10% [17].

4. Calculation of Optical Constants

The scanning electron microscope (SEM) photograph of the measured YAG:Ce phosphor and the particle size distribution data are displayed in Fig. 5. It can be found that the shapes of phosphor particles are nonspherical and vary significantly. SiO_2 particles are added into the phosphor to enhance the light scattering for stronger phosphor absorption of the blue light. The sizes of SiO_2 are normally distributed

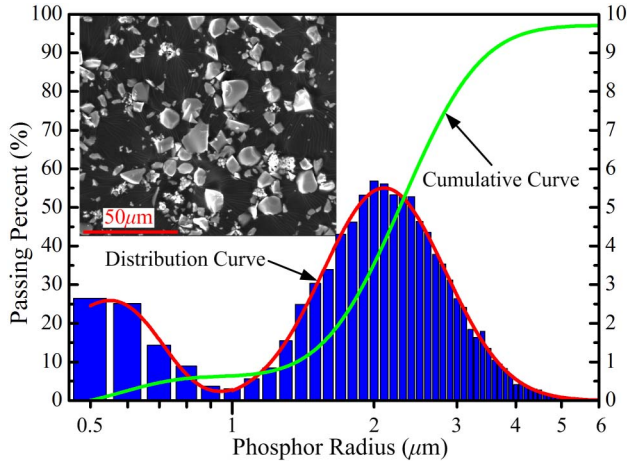

Fig. 5. (Color online) Particle size distribution data and the fitted curves of YAG:Ce phosphor. Inset is a SEM photograph of YAG:Ce phosphor.

from 0.5 to 1 μm and the sizes of phosphor particles are normally distributed from 0.7 to 6 μm. To facilitate the following calculation of the optical constants of the phosphor, the size distribution data are approximated by normal and lognormal functions [27,28].

The size distribution data of SiO_2 are approximated by a normal function $f_s(r)$:

$$f_s(r) = \frac{\varepsilon_s}{\sigma_1\sqrt{2\pi}}\exp\left(-\frac{(r_s-\mu_1)^2}{2\sigma_1^2}\right), \quad (1)$$

where the mean radius μ_1 is 0.55, the standard deviation σ_1 is 0.15, and ε_s is a fitting parameter. Radius r_s is in the range of 0.5–1 μm. The size distribution data of phosphor particles are approximated by a lognormal function $f_{\text{phos}}(r)$:

$$f_{\text{phos}}(r) = \frac{\varepsilon_{\text{phos}}}{r_{\text{phos}}\sigma_2\sqrt{2\pi}}\exp\left(-\frac{(\ln r_{\text{phos}}-\ln\mu_2)^2}{2\sigma_2^2}\right), \quad (2)$$

where the mean radius μ_2 is 2.3, the standard deviation σ_2 is 0.3, and $\varepsilon_{\text{phos}}$ is a fitting coefficient. Radius r_{phos} is in the range of 0.7–6 μm. Therefore, the size distribution function $f(r)$ of the phosphor is expressed as

$$f(r) = f_s(r) + f_{\text{phos}}(r). \quad (3)$$

The cumulative function $F(r)$ is an integration of $f(r)$:

$$F(r) = \int f(r)\mathrm{d}r. \quad (4)$$

$F(r)$ is approximately 1 when r is integrated from 0.5 to 6 μm. Therefore, the particle size distribution has a good description by these approximation functions. It should be noticed that the particle size distribution data for nonspherical particles, such as the phosphor, can be varied by different measurement equipment, test methods, and material samples. Therefore, the approximation functions here are not suitable for all cases.

Since our measurement platform used two color LEDs as the light sources and the true optical constants of the phosphor cannot be directly determined by the measurement results using the many-flux theory, this study applies two steps to obtain precise optical constants of the phosphor. The first step is a Mie theoretical calculation that considers SiO_2 and phosphor particles as spheres and obtains the initial optical constants according to Mie theory. The second step is a Monte Carlo ray-tracing simulation, which constructs the optical model of the measurement platform and approximates the simulation results to the measurement results by adjusting the optical constants based on the Mie theoretical results [27].

A. Mie Theoretical Calculation

According to Mie theory [27,29–35], the optical constants of the phosphor, which are the absorption coefficient $\mu_{abs}(\lambda)$, scattering coefficient $\mu_{sca}(\lambda)$, and anisotropy factor $g(\lambda)$, can be calculated by

$$\mu_{abs}(\lambda) = \int N(r) C_{abs}(\lambda, r) \mathrm{d}r, \tag{5}$$

$$\mu_{sca}(\lambda) = \int N(r) C_{sca}(\lambda, r) \mathrm{d}r, \tag{6}$$

$$g(\lambda) = 2\pi \iint_{-1}^{1} p(\theta, \lambda, r) f(r) \cos\theta \mathrm{d}\cos\theta \mathrm{d}r, \tag{7}$$

where $N(r)$ is the number density distribution of particles (per cubic millimeter), $C_{abs}(\lambda, r)$ and $C_{sca}(\lambda, r)$ are the absorption and scattering cross sections (per square millimeter), $p(\theta, \lambda, r)$ is the phase function, λ is the wavelength of the incident light (nanometers), and θ is the scattering angle.

$N(r)$ is composed of the SiO_2 number density $N_s(r)$ and the phosphor particle number density $N_{phos}(r)$. Theoretically, $N(r)$ has the same curve as $f(r)$, which describes the number density distribution of the unit phosphor. Therefore, for one specific phosphor concentration, $N(r)$ can be calculated by multiplying $f(r)$ with the number density coefficient K_N:

$$N(r) = N_s(r) + N_{phos}(r) = K_N f(r). \tag{8}$$

K_N denotes the number of the unit phosphor for one phosphor concentration. To obtain K_N, we should first know the mass distribution $M(r)$ (milligrams) of the unit phosphor. $M(r)$ can be expressed by

$$M(r) = \rho V(r) f(r) = \frac{4}{3}\pi r^3 [\rho_s f_s(r) + \rho_{phos} f_{phos}(r)], \tag{9}$$

where V is the volume of single particle, ρ_s is the density of SiO_2, and ρ_{phos} is the density of the YAG:Ce crystal. In this calculation, ρ_s and ρ_{phos} are 2.2 and 4.6 mg/mm^3, respectively.

Figure 6 is the calculated curve of $M(r)$. Integrating $M(r)$ can obtain the total mass of the unit phosphor. If the phosphor concentration c (milligrams per cubic millimeter) of the mixture is known, K_N can be obtained by

$$K_N = \frac{c}{\int M(r) \mathrm{d}r}. \tag{10}$$

According to Eq. (10), we find that K_N has a linear relationship with c. This means that $N(r)$ is linearly increased with the increase of c. In Eqs. (5) and (6), theoretically, $C_{abs}(\lambda, r)$ and $C_{sca}(\lambda, r)$ are independent of c. Therefore, as the expected behavior according to the general Kubelka–Munk theory [28,36,37], $\mu_{abs}(\lambda)$ and $\mu_{sca}(\lambda)$ should also have a linear relationship with c. This will be verified in the following calculations.

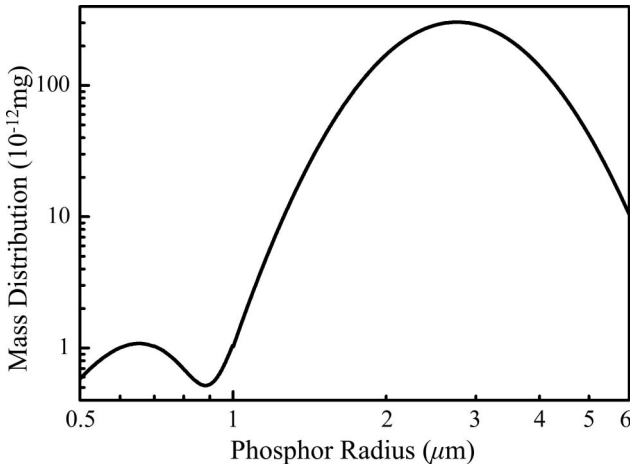

Fig. 6. Mass distribution curve of unit YAG:Ce phosphor.

In Mie theory, $C_{abs}(\lambda, r)$ and $C_{sca}(\lambda, r)$ are normally calculated by the following relations:

$$C_{sca} = \frac{2\pi}{k^2} \sum_{0}^{\infty} (2n+1)(|a_n|^2 + |b_n|^2), \tag{11}$$

$$C_{ext} = \frac{2\pi}{k^2} \sum_{1}^{\infty} (2n+1)\mathrm{Re}(a_n + b_n), \tag{12}$$

$$C_{abs} = C_{ext} - C_{sca}, \tag{13}$$

where C_{ext} is the extinction cross section, k is the wavenumber ($=2\pi/\lambda$), and a_n and b_n are the expansion coefficients with even symmetry and odd symmetry, respectively. a_n and b_n are calculated by

$$a_n = \frac{m\psi_n(mx)\psi_n'(x) - \psi_n'(mx)\psi_n(x)}{m\psi_n(mx)\xi_n'(x) - \psi_n'(mx)\xi_n(x)}, \tag{14}$$

$$b_n = \frac{\psi_n(mx)\psi_n'(x) - m\psi_n'(mx)\psi_n(x)}{\psi_n(mx)\xi_n'(x) - m\psi_n'(mx)\xi_n(x)}, \tag{15}$$

where x is the size parameter ($=kr$), m is the relative refractive index of particles, and $\psi_n(x)$ and $\xi_n(x)$ are the Riccati–Bessel functions.

In the mixture of phosphor and silicone, the refractive index of embedded silicone (n_{sil}) is 1.53, and the refractive index of SiO_2 (n_s) is 1.44. Silicone and SiO_2 both are considered to be transparent for the blue light and the yellow light. The refractive index of the phosphor particle n_{phos} has a complex form:

$$n_{phos} = n'_{phos} - in''_{phos}, \tag{16}$$

where n'_{phos} and n''_{phos} are the real and imaginary refractive indices of the phosphor particle, respectively. Therefore, the relative refractive indices of SiO_2 (m_s) and phosphor (m_{phos}) in the silicone are

$$m_s = n_s/n_{\text{sil}}, \qquad m_{\text{phos}} = n_{\text{phos}}/n_{\text{sil}}. \tag{17}$$

The cross sections of SiO_2 and phosphor particles are separately calculated. Since there is no absorption for the incident light by SiO_2, C_{ext} of SiO_2 will be equal to C_{sca}, and C_{abs} will be zero. For phosphor particles, n'_{phos} is obtained by the following equation:

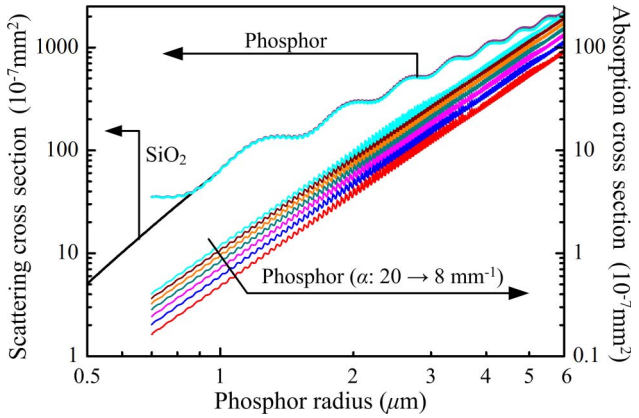

Fig. 7. (Color online) Absorption and scattering cross sections of YAG:Ce phosphor for blue light by Mie theoretical calculation.

$$n' = \sqrt{2.08745 + 1.2081\lambda^2/(\lambda^2 - 0.02119) + 17.2049\lambda^2/(\lambda^2 - 1404.45)}. \tag{18}$$

n''_{phos} is obtained by

$$n'' = \alpha/2k, \tag{19}$$

where α is the absorption coefficient of the phosphor crystal.

Although the optical properties of YAG:Ce crystal have been studied extensively, α varies in a wide range due to the different Ce doping concentrations, crystal growth methods, and measurement equipment [38–42]. The variation of α is normally in the range of 3–8 mm^{-1} for the blue light. But for YAG:Ce optical ceramics, which is composed of small crystal grains, light absorption is significantly enhanced and α can be higher than 15 mm^{-1} [40]. This is due to the multiple internal reflections in the grain, which increases the total light absorption. Considering that the tested phosphor is crystalline powder and can also present high α, this study sets α varied from 8 to 20 mm^{-1} to investigate the variations of $C_{\text{abs}}(455\,\text{nm})$ and $C_{\text{sca}}(455\,\text{nm})$ for the blue light. Figure 7 shows the calculated results of $C_{\text{abs}}(455\,\text{nm})$ and $C_{\text{sca}}(455\,\text{nm})$. According to Eqs. (5), (6), and (10), $\mu_{\text{abs}}(455\,\text{nm})$ and $\mu_{\text{sca}}(455\,\text{nm})$ are calculated and shown in Fig. 8.

From Fig. 7, it can be found that the scattering cross section is one magnitude larger than the absorption cross section, meaning that the phosphor presents strong scattering effect and thereby results in high absorption for the blue light. In Fig. 8, the absorption and scattering coefficients are linearly increased with the increase of the phosphor concentration, indicating that changing the phosphor concentration is a direct approach to control the color of white LEDs. According to the Lambert–Beer law [28,43,44],

$$I = I_0 \exp(-\mu_{\text{ext}} z), \tag{20}$$

where I is the transmitted light power, I_0 is the incident light power, μ_{ext} is the extinction coefficient, and z is the phosphor thickness. μ_{ext} normally has a relation with μ_{abs} and μ_{sca} as [44]

$$\mu_{\text{ext}} = \mu_{\text{abs}} + \mu_{\text{sca}}(1 - g). \tag{21}$$

Therefore, both the increases of the phosphor thickness and the concentration will cause an exponential decrease of I, which is also found in our results in Fig. 3. To make the color of white LED products the same when the phosphor thickness or the

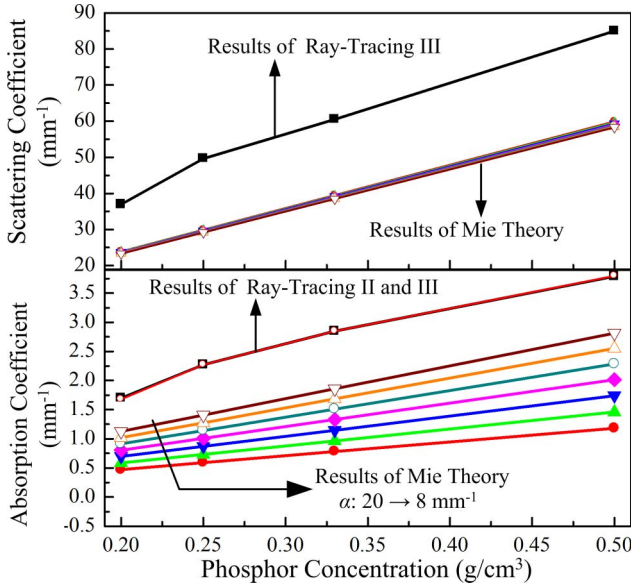

Fig. 8. (Color online) Absorption and scattering coefficients of YAG:Ce phosphor for blue light by Mie theoretical calculation and ray-tracing simulation.

concentration varies, the phosphor concentration or the thickness should be oppositely changed to generate the same I. This will be difficult for white LEDs with very high phosphor concentration, since the phosphor layer may be too thin and may be damaged during the handling.

For the yellow light, α is normally lower than $0.5\,\mathrm{mm}^{-1}$ [38–42]. Like the calculations for the blue light, $C_{\mathrm{abs}}(595\,\mathrm{nm})$, $C_{\mathrm{sca}}(595\,\mathrm{nm})$, $\mu_{\mathrm{abs}}(595\,\mathrm{nm})$, and $\mu_{\mathrm{sca}}(595\,\mathrm{nm})$ are obtained by changing α from 0.1–$0.5\,\mathrm{mm}^{-1}$. The theoretical results are shown in Figs. 9 and 10.

In Figs. 9 and 10, $C_{\mathrm{abs}}(595\,\mathrm{nm})$ and $\mu_{\mathrm{abs}}(595\,\mathrm{nm})$ are almost 3 magnitudes smaller than $C_{\mathrm{sca}}(595\,\mathrm{nm})$ and $\mu_{\mathrm{sca}}(595\,\mathrm{nm})$, meaning that the phosphor absorption for the yellow light is very low and the strong scattering effect is the dominant factor affecting the light output. Comparing Figs. 7 and 8 with Figs. 9 and 10, it can be found that variations of $C_{\mathrm{sca}}(\lambda)$ and $\mu_{\mathrm{sca}}(\lambda)$ are very small when the incident light is changed from the blue light to the yellow light. This indicates that the scattering properties of phosphor in the whole visible light are similar and it is the variation of the absorption properties for different light generating the differences of Figs. 3(a) and 3(b).

The final optical constant that should be determined is $g(\lambda)$, for which the phase function should be first obtained. For small spheres, the phase function $p(\theta,\lambda,r)$ can be calculated according to [30,32]

$$p(\theta,\lambda,r)=\frac{4\pi\beta(\theta,\lambda,r)}{k^2C_{\mathrm{sca}}(\lambda,r)}, \tag{22}$$

where $\beta(\theta,\lambda,r)$ is the dimensionless scattering function, which is obtained by the scattering amplitude functions $S_1(\theta)$ and $S_2(\theta)$:

$$\beta(\theta)=(1/2)[|S_1(\theta)|^2+|S_2(\theta)|^2], \tag{23}$$

$$S_1(\theta)=\sum_{n=1}^{\infty}\frac{2n+1}{n(n+1)}\left[a_n\frac{P_n^1(\cos\theta)}{\sin\theta}+b_n\frac{\mathrm{d}P_n^1(\cos\theta)}{\mathrm{d}\theta}\right], \tag{24}$$

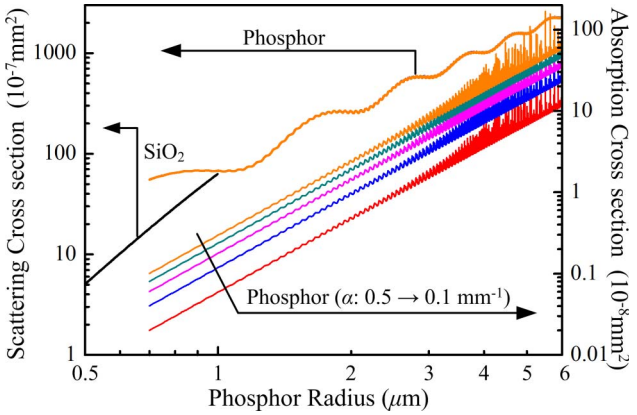

Fig. 9. (Color online) Absorption and scattering cross sections of YAG:Ce phosphor for yellow light by Mie theoretical calculation.

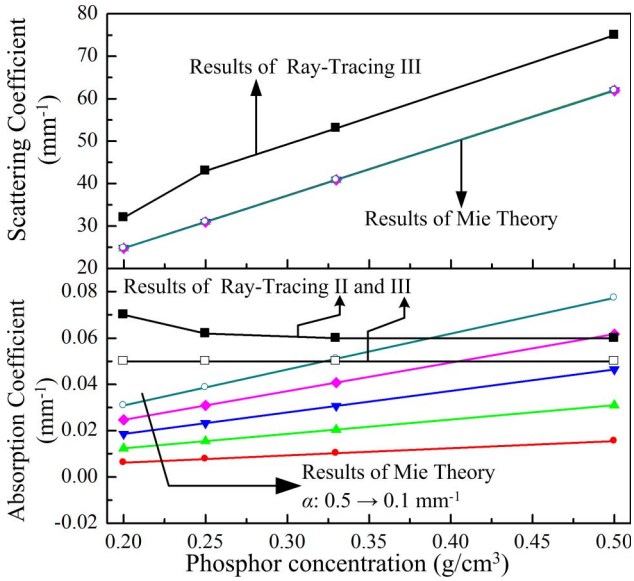

Fig. 10. (Color online) Absorption and scattering coefficients of YAG:Ce phosphor for yellow light by Mie theoretical calculation and ray-tracing simulation.

$$S_2(\theta)=\sum_{n=1}^{\infty}\frac{2n+1}{n(n+1)}\left[b_n\frac{P_n^1(\cos\theta)}{\sin\theta}+a_n\frac{\mathrm{d}P_n^1(\cos\theta)}{\mathrm{d}\theta}\right], \tag{25}$$

where ${P^1}_n(\cos\theta)$ is the associated Legendre polynomial.

According to Eq. (7), the theoretical results of $g(\lambda)$ are calculated and shown in Fig. 11. Results show that the variation of α has slight impact on g, and the increase of $g(\lambda)$ by α is so small that the increase can be neglected. Therefore, the theoretically reasonable values of $g(455\,\mathrm{nm})$ and $g(595\,\mathrm{nm})$ are around 0.90 and 0.89, respectively. A point that should be noticed is that $g(595\,\mathrm{nm})$ is a little lower than $g(455\,\mathrm{nm})$. Generally, the anisotropy factor of particles for a long wavelength should be larger than that for a short wavelength. It means that the particles should present stronger a scattering effect for a short wavelength. This theoretical result will be modified in the following ray-tracing simulation.

B. Ray-Tracing Simulation

In the optical model of the measurement platform, the blue light or the yellow light is emitted from the top surface of the chip with a Lambertian radiation pattern. The material of the lenses is BK7 from Schott. The inner surfaces of the two integrating spheres are coated with a diffuse white material having optical properties of 11.1% absorption and 89.9% scattering. The support glass of the phosphor slide is also BK7 glass. The inner surfaces of the integrating spheres are used as the receivers to collect the transmitted and reflected light.

The Monte Carlo method is applied for the ray tracing of the optical model. Phosphor is considered to

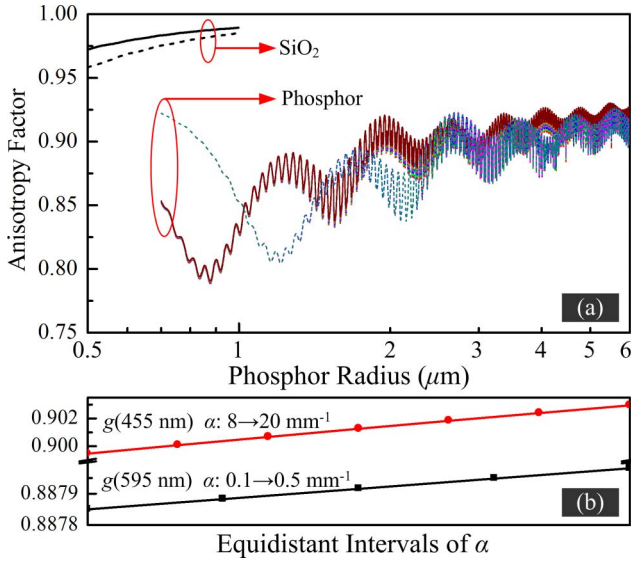

Fig. 11. (Color online) Anisotropy factors of YAG:Ce phosphor for (a) single particle scattering and (b) volume scattering by Mie theoretical calculation. Solid curves in (a) are the results for blue light and dashed curves are the results for yellow light.

be a Mie scattering material. Since the ray tracing cannot directly compute the scattering directions of the light in the phosphor, the Henyey–Greenstein function is used as an approximation of the generation of the angular scattering. This function is [29,30]

$$p(\theta) = \frac{1-g^2}{4\pi(1-2g\cos\theta+g^2)^{3/2}}, \qquad (26)$$

where g is obtained from the results of Fig. 11.

We first applied the Mie theoretical results with no change in the optical model. However, the ray-tracing results showed that the transmittance was significantly higher than that of the measurement results and the absorption for the blue light was lower than that of the measurement results. Three reasons result in these differences. They are the lower $\mu_{abs}(\lambda)$, lower $\mu_{sca}(\lambda)$, and higher $g(\lambda)$, when comparing with the true values. Therefore, three methodologies were adopted in the following simulations to obtain more precise optical constants. The methodologies were keeping one of three constants unchanged in sequence and at the same time adjusting the other two constants to approximate the measurement results. We denoted the three methodologies as ray-tracing I, II, and III.

In ray-tracing I, $\mu_{abs}(\lambda)$ was unchanged. According to Eqs. (20) and (21), changing $\mu_{sca}(\lambda)$ and $g(\lambda)$ can make the transmitted light approximate the measurement results. We found that increasing $\mu_{sca}(\lambda)$ or lowering $g(\lambda)$ can realize similar transmittance as the measurement results, but the reflectance is always larger than that of the measurement results. If the reflectance has a good match with that of measurement results, the transmittance will be larger. The errors between the ray-tracing results and the measurement results can be larger than 10% in some thicknesses and concentrations of the phosphor. This means that $\mu_{abs}(\lambda)$ of Mie results is smaller than the actual value and cannot generate enough phosphor absorption for the incident light.

In ray-tracing II, $\mu_{abs}(\lambda)$ and $g(\lambda)$ were changed. Since the variations of $\mu_{sca}(\lambda)$ of Mie results by α are small, the ray-tracing simulation chose the average value as the initial $\mu_{sca}(\lambda)$. By adjusting $\mu_{abs}(\lambda)$ and $g(\lambda)$, the optical approximation can reduce the errors between the ray-tracing results and the measurement results to be smaller than 5% for all phosphor thicknesses and concentrations. The modified $\mu_{abs}(\lambda)$ and $g(\lambda)$ are shown in Figs. 8, 10, and 12. From Fig. 8, it can be seen that the change of $\mu_{abs}(455\,\text{nm})$ of the ray-tracing results shows a similar tendency as that of the Mie theoretical results with $\alpha = 20\,\text{mm}^{-1}$. For the yellow light, the tendency of $\mu_{abs}(595\,\text{nm})$ of the ray-tracing results cannot present a good match with that of the Mie results. This may be because the phosphor absorption for the yellow light is very low and the strong scattering effect weakens the differences of the phosphor absorption in different phosphor concentrations. This causes the slight changes of $\mu_{abs}(595\,\text{nm})$ of the ray-tracing results, as shown in Fig. 10. Comparing with Fig. 8, we believed that a reasonable value of α for the yellow light is in the range of 0.2–0.4 mm^{-1}. Figure 12 gives $g(\lambda)$ of the ray-tracing results, which is lower than that of the Mie theoretical results. Unlike the Mie results, it can be found that $g(595\,\text{nm})$ is higher than $g(455\,\text{nm})$ in the ray-tracing results. This is more reasonable for the actual light scattering.

In Fig. 12, there is a sudden decrease of $g(\lambda)$ at the concentration of 0.25 g/cm^3. $\mu_{abs}(\lambda)$ also shows a small decrease at the concentration of 0.20 g/cm^3 in Figs. 8 and 10. This may be caused by the test errors and local inhomogeneity of the phosphor powder in the samples. When the phosphor concentration decreases, the local inhomogeneity has more significant effects on the light scattering and causes variations of $g(\lambda)$ and $\mu_{abs}(\lambda)$ similar to the ray-tracing results.

In ray-tracing III, $g(\lambda)$ was unchanged. The ray-tracing simulation set $g(455\,\text{nm})$ and $g(595\,\text{nm})$ to be 0.9 and 0.89, respectively. By controlling the errors between the ray-tracing results and the measurement results to be smaller than 5%, the modified $\mu_{abs}(\lambda)$ and $\mu_{sca}(\lambda)$ are shown in Figs. 8 and 10. It can be found that $\mu_{sca}(\lambda)$ of the ray-tracing results

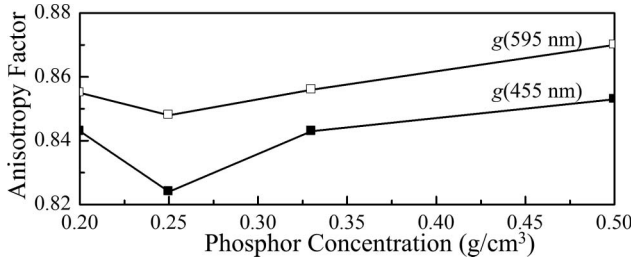

Fig. 12. Ray-tracing results of anisotropy factor of YAG:Ce phosphor by ray-tracing simulation.

presents a tendency similar to that of the Mie results, but the values are higher. Another point that should be noted is that the differences of $\mu_{abs}(\lambda)$ between the results of ray-tracing II and III are very small. This indicates that, when the absorption property of the phosphor has been correctly determined, both the change of $\mu_{sca}(\lambda)$ and $g(\lambda)$ can realize the same light-scattering effects.

Therefore, according to Eq. (21), a reduced scattering coefficient $\delta_{sca} = \mu_{sca}(1-g)$ is introduced to describe the scattering property of the phosphor to give better comparisons of the Mie results and the ray-tracing results. The comparisons are shown in Fig. 13. It can be seen that the values of δ_{sca} in the results of ray-tracing II and III are almost coincident, implying that δ_{sca} is more precise in the description of the light scattering of the phosphor. Results also show that $\delta_{sca}(595\,\text{nm})$ is larger than $\delta_{sca}(455\,\text{nm})$ in the Mie theoretical results but smaller than $\delta_{sca}(455\,\text{nm})$ in the ray-tracing results. This means that Mie theory is not accurate enough in the description of the scattering property of the phosphor when the incident light changes from the excitation spectra to the emission spectra. In addition, the differences between $\delta_{sca}(455\,\text{nm})$ and $\delta_{sca}(595\,\text{nm})$ in the ray-tracing results are smaller than those in the Mie theoretical results. Therefore, the scattering property of the phosphor in the whole visible spectra will be similar.

Finally, a precise result of the optical constants of the phosphor material has been obtained by the ray-tracing simulation. This ray-tracing simulation also provides a rough estimation method of the optical constants of YAG:Ce phosphor. From Figs. 8 and 13, it can be found that both $\mu_{abs}(\lambda)$ and $\delta_{abs}(\lambda)$ of the ray-tracing results are generally larger than those of the Mie theoretical results. For the blue light, the ratios of $\mu_{abs}(455\,\text{nm})$ between the ray-tracing results and the Mie theoretical results are normally around 1.47, and the ratios of $\delta_{abs}(455\,\text{nm})$ are normally around 1.63. For the yellow light, the actual values

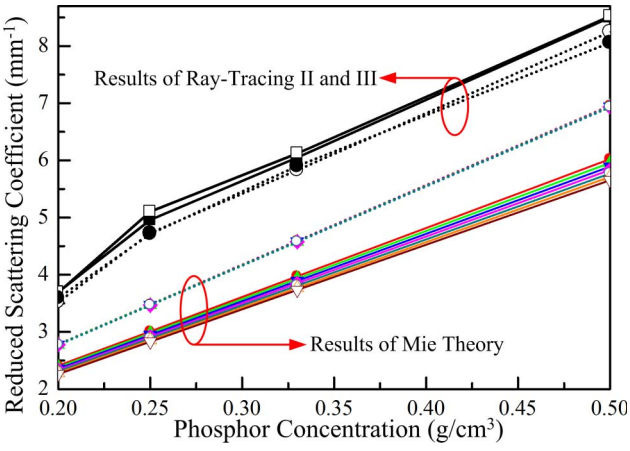

Fig. 13. (Color online) Comparisons of reduced scattering coefficients between ray-tracing results and Mie theoretical results. Solid and dashed curves are the results for blue light and yellow light, respectively.

of $\delta_{sca}(595\,\text{nm})$ are a little lower than those of $\delta_{sca}(455\,\text{nm})$ of the ray-tracing results, and the ratios between the ray-tracing results and the Mie theoretical results are normally around 1.27. The actual values of $\mu_{abs}(595\,\text{nm})$ are almost the same and can be defined to be a very low value, according to Fig. 10. Therefore, in the optical design of white LED packaging, the optical constants of YAG:Ce phosphor can be roughly obtained by multiplying Mie theoretical results with these ratios.

5. Revised Mie Calculation of Optical Constants

As a prospect, the Mie theoretical results and the ray-tracing results are further discussed here to find whether the Mie theory can be revised by a simple method to give a more precise description of the phosphor optical properties. This is because Mie theory is widely used in most commercial optical software, such as Lighttools, Tracepro, and ASAP, which normally treat the phosphor scattering as Mie scattering to realize the optical simulation of white LED packaging. Revised Mie calculation of the optical constants can provide reasonable supports in the optical simulation and make the software more powerful in LED packaging design.

In the final part of Section 4, the ratio coefficients are declared to modify the Mie theoretical results. This is not accurate enough from the theoretical view. The real reason for the differences between the Mie theoretical results and the ray-tracing results is that the extinction cross section of Mie theory is smaller than the actual cross section. With the size distribution data used in Mie theory, it is difficult to reflect the true sizes of phosphor particles due to their nonspherical shapes. Therefore, the method of treating nonspherical phosphor particles to be spheres by Mie theory reduces the actual extinction cross section. A simple method is modifying $C_{abs}(\lambda)$ and $C_{sca}(\lambda)$ by two fitting parameters k_{abs} and k_{sca} as

$$C'_{abs} = k_{abs}C_{abs}, \qquad C'_{sca} = k_{sca}C_{sca}. \tag{27}$$

According to Eqs. (5)–(7) and (22), $\mu_{abs}(\lambda)$, $\mu_{sca}(\lambda)$, and $g(\lambda)$ will be revised to be

$$\mu'_{abs} = k_{abs}\mu_{abs}, \qquad \mu'_{abs} = k_{sca}\mu_{sca}, \qquad g' = g/k_{sca}. \tag{28}$$

Therefore, $\delta_{sca}(\lambda)$ will be revised to be

$$\delta'_{sca} = k_{sca}\mu_{sca}(1-g/k_{sca}) = \mu_{sca}(k_{sca}-g), \tag{29}$$

where C'_{abs}, C'_{sca}, μ'_{abs}, μ'_{sca}, g', and δ'_{sca} are the revised optical constants including the absorption cross section, scattering cross section, absorption coefficient, scattering coefficient, anisotropy factor, and reduced scattering coefficient, respectively.

If k_{abs} and k_{sca} can be determined by some measurement systems, for example, 45/0 geometry with a daylight lamp [28], a spectrofluorimeter with a white light source and a yellow filter [43], and the

double-integrating-sphere system here, the revised Mie calculation will give a precise prediction of the phosphor optical properties. In our experiments, k_{abs} for the blue light is around 1.47. k_{sca} for the blue light and yellow light are around 1.06 and 1.03, respectively. Therefore, Mie theory has a good description of the phosphor scattering but has difficulty in the description of the phosphor absorption.

This revised Mie calculation method also makes the optical constants of YAG:Ce phosphor more simply obtained by studying white LEDs with different phosphor concentrations. Kang *et al.* [24] first theoretically studied the optical model of white LEDs by Lambert-Beer law and gave the optical constants of the phosphor by their white LED samples. The theoretical method developed by Kang *et al.* [24] is effective but not precise enough, since the multiple reflection discussed in Section 2 was not seriously considered in their studies. This causes the optical constants to be larger than the actual values. Combining the revised Mie calculation with their method can reduce the calculation errors. Finally, the ray-tracing simulation should also be applied to examine the optical model of white LED to determine the correction of k_{abs} and k_{sca}.

6. Conclusion

A measurement of the optical properties of YAG:Ce phosphor was conducted by the double-integrating-sphere system. The measurement results revealed the factors affecting the optical performance of white LEDs by the phosphor. Generally, the strong scattering for the yellow light and the isotropic emission pattern are the main factors and have prompted great efforts to eliminate their adverse effects. Because the light sources in our measurement platform were two color LEDs, rather than monochromatic light, both Mie theoretical calculation and Monte Carlo ray-tracing simulation were used to obtain precise optical constants of the phosphor, including the absorption coefficient, scattering coefficient, and anisotropy factor. Numerical results showed that Mie theory is effective in the prediction of the tendencies of the optical constants as the phosphor concentration changes. However, the method of treating nonspherical phosphor particles to be spheres causes the absorption and scattering cross sections to be smaller than the actual cross sections. Revisions of the absorption and scattering cross sections with two fitting parameters can improve the accuracy of Mie theoretical results and make the Mie theory suitable for the optical design of LED packaging. The fitting parameters can be obtained by a measurement of the optical properties of phosphor films or a numerical analysis of white LEDs with various phosphor concentrations. This study only obtains the fitting parameters for the two color LEDs. From the view of a complete and correct measurement, the light source should use a daylight source that is sampled by a monochromator to generate monochromatic light covering the visible spectra range [28,43], and this will be our future work.

This work was supported by the Nature Science Foundation of China (NSFC) Key Project under grant 50835005, NSFC Project under grant 50876038, and High Technology Project of the Ministry of Science and Technology under grant 2008AA03A184. The authors would also like to thank the Science and Technology Department of Guangdong Province and Guangdong Real Faith Enterprises Group Co. Ltd. for their support.

References

1. E. F. Schubert and J. K. Kim, "Solid-state light source getting smart," Science **308**, 1274–1278 (2005).
2. J. K. Kim and E. F. Schubert, "Transcending the replacement paradigm of solid-state lighting," Opt. Express **16**, 21835–21842 (2008).
3. D. A. Steigerwald, J. C. Bhat, D. Collins, R. M. Fletcher, M. O. Holcomb, M. J. Ludowise, P. S. Martin, and S. L. Rudaz, "Illumination with solid state lighting technology," IEEE J. Sel. Top. Quantum Electron. **8**, 310–320 (2002).
4. M. R. Krames, O. B. Shchekin, R. Mueller-Mach, G. O. Mueller, L. Zhou, G. Harbers, and M. G. Craford, "Status and future of high-power light-emitting diodes for solid-state lighting," J. Display Technol. **3**, 160–175 (2007).
5. P. Schlotter, R. Schmidt, and J. Schneider, "Luminescence conversion of blue light emitting diodes," Appl. Phys. A **64**, 417–418 (1997).
6. K. Sakuma, K. Omichi, N. Kimura, M. Ohashi, D. Tanaka, N. Hirosaki, Y. Yamamoto, R.-J. Xie, and T. Suehiro, "Warm-white light-emitting diode with yellowish orange SiAlON ceramic phosphor," Opt. Lett. **29**, 2001–2003 (2004).
7. H. Wu, X. Zhang, C. Guo, J. Xu, M. Wu, and Q. Su, "Three-band white light from InGaN-based blue LED chip precoated with green/red phosphors," IEEE Photonics Technol. Lett. **17**, 1160–1162 (2005).
8. S. Nakamura, S. Pearton, and G. Fasol, *The Blue Laser Diode: GaN Based Light Emitters and Lasers*, 2nd ed. (Springer, 1997), pp. 215–230.
9. R. Mueller-Mach, G. O. Mueller, M. R. Krames, and T. Trottier, "High-power phosphor-converted light-emitting diodes based on III-nitrides," IEEE J. Sel. Top. Quantum Electron. **8**, 339–345 (2002).
10. R. Mueller-Mach, G. Mueller, M. R. Krames, H. A. Hoppe, F. Stadler, W. Schnick, T. Juestel, and P. Schmidt, "Highly efficient all-nitride phosphor-converted white light emitting diode," Phys. Status Solidi **202**, 1727–1732 (2005).
11. R. J. Xie, N. Hirosaki, K. Sakuma, and N. Kimura, "White light-emitting diodes (LEDs) using (oxy)nitride phosphors," J. Phys. D **41**, 144013 (2008).
12. M. Zachau, D. Becker, D. Berben, T. Fiedler, F. Jermann, and F. Zwaschka, "Phosphors for solid state lighting," Proc. SPIE **6910**, 691010 (2008).
13. Z. Liu, S. Liu, K. Wang, and X. Luo, "Status and prospect for phosphor-based white light-emitting diodes packaging," Front. Optoelectron. China **2**, 119–140 (2009).
14. H. Luo, J. K. Kim, E. F. Schubert, J. Cho, C. Sone, and Y. Park, "Analysis of high-power packages for phosphor-based white-light-emitting diodes," Appl. Phys. Lett. **86**, 243505 (2005).
15. S. C. Allen and A. J. Steckl, "ELiXIR-solid-state luminaire with enhanced light extraction by internal reflection," J. Display Technol. **3**, 155–159 (2007).
16. S. C. Allen and A. J. Steckl, "A nearly ideal phosphor-converted white light-emitting diode," Appl. Phys. Lett. **92**, 143309 (2008).

17. Z. Y. Liu, S. Liu, K. Wang, and X. B. Luo, "Optical analysis of phosphor's location for high-power light-emitting diodes," IEEE Trans. Device Mater. Reliab. **9**, 65–73 (2009).
18. N. Narendran, F. Gu, J. P. Freyssinier-Nova, and Y. Zhu, "Extracting phosphor-scattered photons to improve white LED efficiency," Phys. Status Solidi **202**, R60–R62 (2005).
19. N. T. Tran and F. G. Shi, "Studies of phosphor concentration and thickness for phosphor-based white light-emitting-diodes," J. Lightwave Technol. **26**, 3556–3559 (2008).
20. L. Wang, P. F. Gu, and S. Z. Jin, "Enhancement of flip-chip white light-emitting diodes with a one-dimensional photonic crystal," Opt. Lett. **34**, 301–303 (2009).
21. C. Sommer, F. P. Wenzl, P. Hartmann, P. Pachler, M. Schweighart, and G. Leising, "Tailoring of the color conversion elements in phosphor-converted high-power LEDs by optical simulations," IEEE Photon. Technol. Lett. **20**, 739–741 (2008).
22. Z. Y. Liu, S. Liu, K. Wang, and X. B. Luo, "Optical analysis of color distribution in white LEDs with various packaging methods," IEEE Photon. Technol. Lett. **20**, 2027–2029 (2008).
23. Y. Zhu, N. Narendran, and Y. Gu, "Investigation of the optical properties of YAG:Ce phosphor," Proc. SPIE **6337**, 63370S (2006).
24. D.-Y. Kang, E. Wu, and D.-M. Wang, "Modeling white light-emitting diodes with phosphor layers," Appl. Phys. Lett. **89**, 231102 (2006).
25. J. W. Pickering, S. A. Prahl, N. v. Wieringen, J. F. Beek, H. J. C. M. Sterenborg, and M. J. C. van Gemert, "Double-integrating-sphere system for measuring the optical properties of tissue," Appl. Opt. **32**, 399–410 (1993).
26. A. N. Yaroslavsky, I. V. Yaroslavsky, T. Goldbach, and H. J. Schwarzmaier, "Influence of the scattering phase function approximation on the optical properties of blood determined from the integrating sphere measurements," J Biomed. Opt. **4**, 47–53 (1999).
27. M. I. Mishchenko, J. W. Hovenier, and L. D. Travis, *Light Scattering by Nonspherical Particles: Theory, Measurements, and Applications* (Academic, 2000).
28. H. G. Volz, *Industrial Color Testing: Fundamentals and Techniques* (Wiley-VCH, 2001).
29. C. F. Bohren and D. R. Huffman, *Absorption and Scattering of Light by Small Particles* (Wiley, 1983), pp. 57–129.
30. M. Jonasz and G. R. Fournier, *Light Scattering by Particles in Water* (Elsevier, 2007), pp. 87–130.
31. A. R. Jones, "Light scattering for particle characterization," Prog. Energy Combust. Sci. **25**, 1–53 (1999).
32. M. I. Mishchenko, L. D. Travis, and A. A. Lacis, *Scattering, Absorption, and Emission of Light by Small Particles* (Cambridge U. Press, 2004).
33. M. I. Mishchenko, L. D. Travis, R. A. Kahn, and R. A. West, "Modeling phase functions for dustlike tropospheric aerosols using a shape mixture of randomly oriented polydisperse spheroids," J. Geophys. Res. **102**, 16831–16847 (1997).
34. M. I. Mishchenko, J. W. Hovenier, and D. W. Mackowski, "Singe scattering by a small volume element," J. Opt. Soc. Am. A **21**, 71–87 (2004).
35. M. I. Mishchenko, L. D. Travis, and A. Macke, "Scattering of light by polydisperse, randomly oriented, finite circular cylinders," Appl. Opt. **35**, 4927–4940 (1996).
36. D. M. Hembree and H. R. Smyrl, "Anomalous dispersion effects in diffuse reflectance infrared Fourier transform spectroscopy: a study of optical geometries," Appl. Spectrosc. **43**, 267–274 (1989).
37. M. K. Gunde and Z. C. Orel, "Absorption and scattering of light by pigment particles in solar-absorbing paints," Appl. Opt. **39**, 622–628 (2000).
38. S. M. Kaczmarek, G. Domianiak-Dzik, W. Ryba-Romanowski, J. Kisielewski, and J. Wojtkowska, "Changes in optical properties of Ce:YAG crystals under annealing and irradiation processing," Cryst. Res. Technol. **34**, 1031–1036 (1999).
39. M. Kucera, P. Hasa, and J. Hakenov, "Optical and magneto-optical properties of Ce: YAG," J. Alloys Compd. **451**, 146–148 (2008).
40. E. Mihokova, M. Nikl, J. A. Mares, A. Beitlerov, A. Vedda, K. Nejezchleb, K. Blazek, and C. D'Ambrosio, "Luminescence and scintillation properties of YAG:Ce single crystal and optical ceramics," J. Lumin. **126**, 77–80 (2007).
41. G. J. Zhao, X. H. Zeng, J. Xu, S. M. Zhou, and Y. Z. Zhou, "Temperature gradient technique (TGT) growth and characterizations of large-sized Ce-doped YAG scintillation crystal," Phys. Status Solidi A **199**, 355–359 (2003).
42. J. A. Mares, A. Beitlerova, M. Nikl, N. Solovieva, K. Nitsch, M. Kucera, M. Kubova, V. Gorbenko, and Y. Zorenko, "Scintillation and optical properties of YAG:Ce films grown by liquid phase epitaxy," Radiat. Meas. **42**, 533–536 (2007).
43. G. Sharma, *Digital Color Imaging Handbook* (CRC, 2003).
44. A. Ishimaru, *Wave Propagation and Scattering in Random Media* (Academic, 1999).